

Sediment Characteristics of Mergui Basin, Andaman Sea based on Multi-proxy Analyses

Karakteristik Sedimen Cekungan Mergui, Laut Andaman berdasarkan Analisis Multi-proksi

Rina Zuraida¹, Rainer A. Troa², Marfasran Hendrizen³, Luli Gustiantini¹, and Eko Triarso²

¹ Marine Geological Institute of Indonesia, Jl. Dr. Junjunan No. 236 Bandung, Telp: (022) 6032020, Fax: (022) 6017887

² Marine Research Center (MRC), ARHRMF, Ministry of Marine Affairs and Fisheries

³ Research Center for Geotechnology, LIPI, Bandung

Corresponding author : rina@mgi.esdm.go.id

(Received 30 October 2017; in revised from 01 November 2017; accepted 07 February 2018)

ABSTRACT: This paper presents the characteristics of sediment from core BS-36 (6°55.85' S and 96°7.48' E, 1147.1 m water depth) that was acquired in the Mergui Basin, Andaman Sea. The analyses involved megascopic description, core scanning by multi-sensor core logger, and carbonate content measurement. The purpose of this study is to determine the physical and chemical characteristics of sediment to infer the depositional environment. The results show that this core can be divided into 5 lithologic units that represent various environmental conditions. The sedimentation of the bottom part, Units V and IV were inferred to be deposited in suboxic to anoxic bottom condition combined with high productivity and low precipitation. Unit III was deposited during high precipitation and oxic condition due to ocean ventilation. In the upper part, Units II and I occurred during higher precipitation, higher carbonate production and suboxic to anoxic condition.

Keywords: sediment characteristics, Mergui Basin, Andaman Sea, suboxic, anoxic, oxic, carbonate content

ABSTRAK: Makalah ini menyajikan karakteristik sedimen contoh inti BS-36 (6°55,85' LS dan 96°7,48' BT, kedalaman 1147,1 m) yang diambil di Cekungan Mergui, Laut Andaman. Metode analisis meliputi pemerian megaskopis contoh inti, pemindaian contoh inti dengan menggunakan multi-sensor core logger, dan pengukuran kandungan karbonat. Tujuan penelitian adalah untuk mengetahui karakteristik fisik dan kimiawi sedimen untuk menafsirkan kondisi lingkungan pengendapan. Hasil penelitian menunjukkan bahwa contoh inti ini dapat dibagi menjadi 5 unit litologi yang mewakili kondisi lingkungan yang berbeda. Pada bagian bawah sedimen, Unit V dan IV ditafsirkan sebagai hasil endapan pada kondisi suboksik hingga anoksik pada saat produktivitas tinggi dan curah hujan rendah. Unit III didapatkan pada saat curah hujan tinggi dan kondisi oksik yang diperkirakan berkaitan dengan ventilasi samudera. Pada bagian atas, Unit II dan I didapatkan pada saat curah hujan cukup tinggi dengan produksi karbonat yang cukup besar dan kondisi dasar laut suboksik hingga anoksik.

Kata kunci: karakteristik sedimen, Cekungan Mergui, Laut Andaman, suboksik, anoksik, oksik, kandungan karbonat

INTRODUCTION

Marine sediment is an accumulation of detrital, biogenic, and authigenic particles that are deposited at the seafloor. Detrital particles are mostly derived from continental or terrestrial weathering (Millot, 1970) which reflect their source rocks (Hemming *et al.*, 2007). Biogenic particles that are found in marine sediments are mostly carbonate tests of microorganism such as foraminifera (Hansen, 1999 in Gupta, 1999; Rahman and Oomori, 2008) or siliceous shells radiolaria (Anderson, 1983). Changes in the environment would

be reflected in microorganism assemblages, particularly foraminifera. Thus foraminiferal assemblage could be used to reconstruct environmental condition as have been reported by e.g. Spooner *et al.* (2005) from Banda Sea, and Gustiantini *et al.* (2015) from Halmahera Sea. Authigenic particles are *in situ* precipitates which formation are influenced by environmental condition (Boles, 2014). Therefore, authigenic particle could be used to detect environmental condition during deposition, such as the level of sea bottom oxygenation (Kraal *et al.*, 2012).

Andaman Sea that is located to the north of Sumatra connects Malacca Strait to the Indian Ocean. Andaman Sea is bounded on the west by Thailand and Myanmar and to the northwest by Indian subcontinent. Previous study from this region showed that Andaman Sea is strongly influenced by *Indian Ocean Monsoon* (Rashid *et al.*, 2007) as well as shifting of the locus of Asian summer monsoon (Awasthi *et al.*, 2014). To date, most of published studies have been concentrated in the eastern part of Andaman Basin (Figure 1), while scarce data comes from Mergui Basin that is located in the southern part of Andaman Sea. This study provides new data on physical and chemical characteristics of the study area (Figure 1). Our finding is the first step towards understanding environmental changes in this region.

Geology and Oceanography of Andaman Sea

Andaman Sea is separated from the Indian Ocean by Andaman-Nicobar island arcs. The bathymetry of Andaman Sea ranges between 200 and 2500 m and the deepest bathymetry is located in the central part of East Andaman Basin (Figure 1, right). The southeast part of Andaman Sea is occupied by Mergui Basin that connects the Sea to Sunda Shelf. Mergui Basin is characterized by gentle slope to the east and north and steep slope to the south (maximum slope is 83) and

eastward-bearing channel that connect Mergui Basin with Andaman Basin (Figure 1, right). The water depth of Mergui Basin ranges between 400 and 1700 m and the maximum depth is located at the edge of Andaman Basin (Troa *et al.*, 2014).

Mergui Basin is formed by post-Oligocene normal fault with annual subsidence rate of 0.25 mm/year. That rate of subsidence allows sediment supply from mainland Asia, Sumatra and Sunda Shelf to be deposited in the basin (Lin *et al.*, 2010). One of the factor that controls sediment supply to Sunda Shelf is the vast topographical difference between mainland Asia and Indonesia archipelago (Hall and Morley, 2004). In addition to terrigenous fragments from surrounding lands, marine sediment of Mergui Basin is also composed of biogenic particles such as foraminifera, pteropod and radiolaria (Tripathi, 2014).

Oceanography modelling in Malacca Strait and Andaman Sea on long-term data shows slight different in current that flows in the study area during Northeast (NE) Monsoon and Southwest (SW) Monsoon (Rizal *et al.*, 2012). Even though the general current direction only shows slight seasonal changes, a counter-current is observed flowing to the southeast during NE Monsoon (Figure 2). The general circulation pattern indicates shifting of ocean front from Malacca Strait with strongest flow during NE Monsoon that pushes the

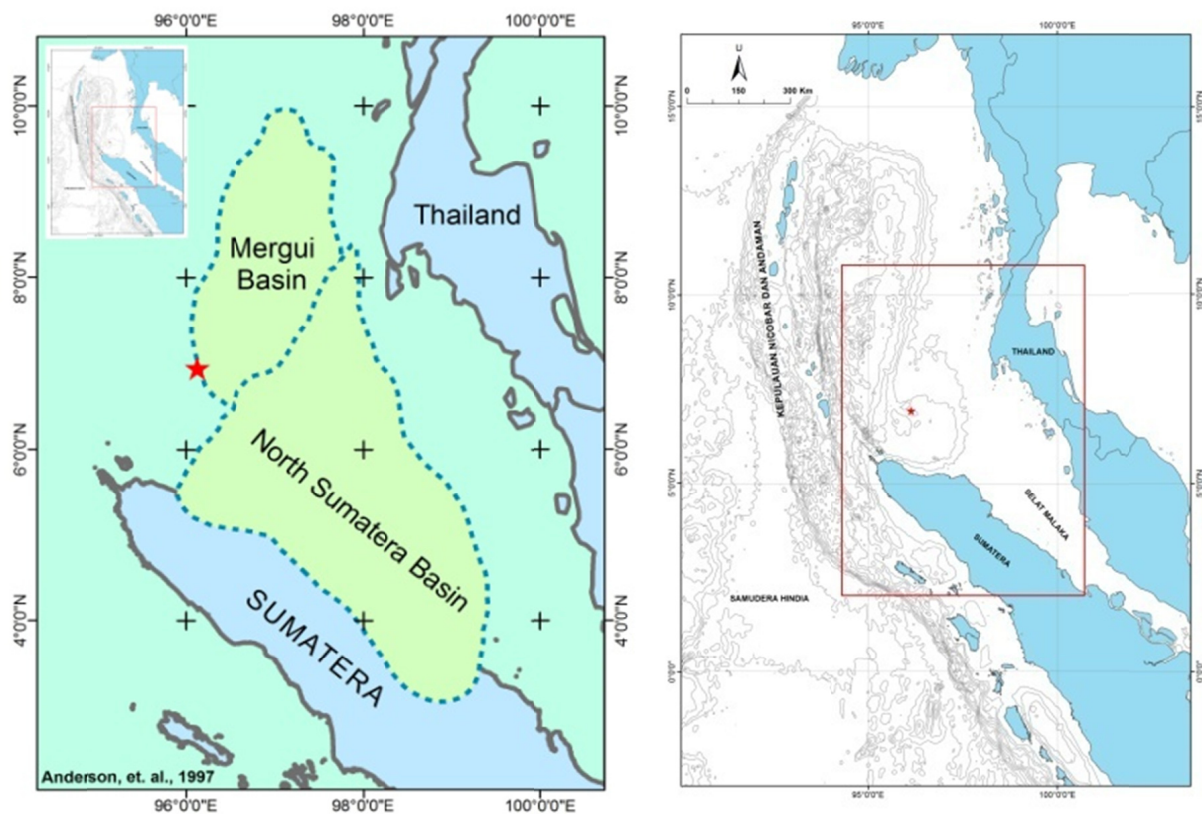


Figure 1. Left: location of Core BS-36 that was acquired near the edge of Mergui Basin (red star). Map source: Anderson *et al.* (1997 in Razali, 2011). Right: bathymetry surrounding Core BS-36 (Troa *et al.*, 2014).

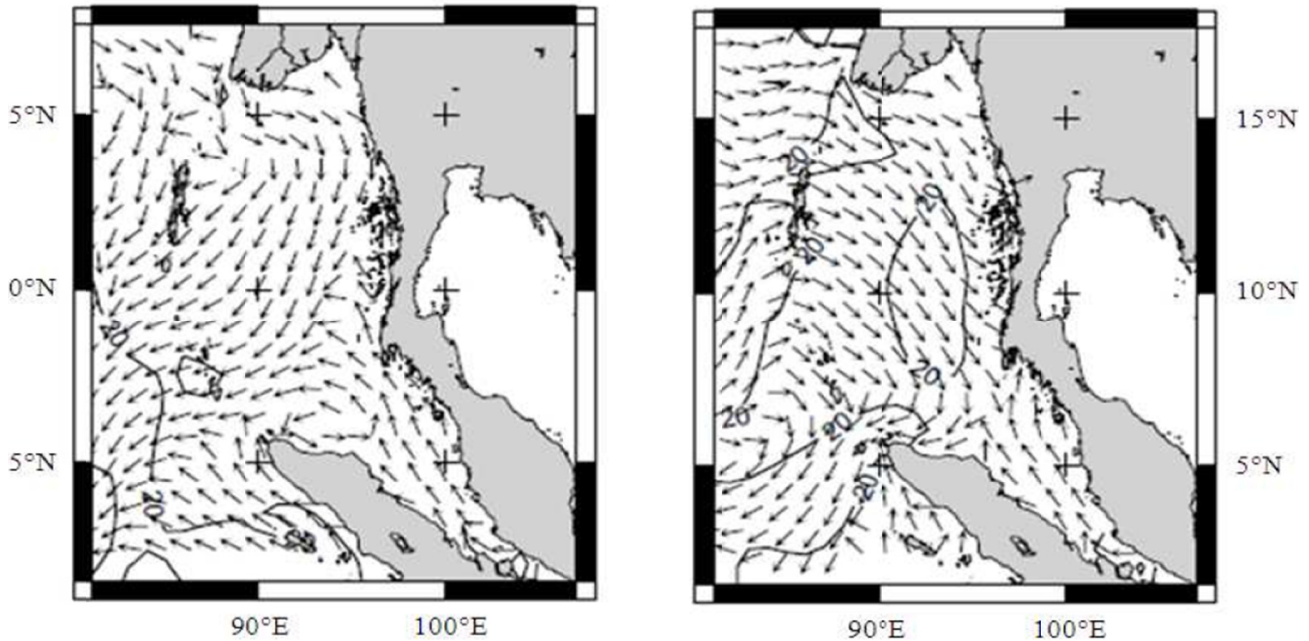


Figure 2. Circulation pattern in Andaman Sea and Malacca Strait based on long-term current modeling. Left: December–February during northeast monsoon, right: June - September during southwest monsoon (Rizal *et al.*, 2012).

Indian Ocean water to the northern border of the Andaman Basin (Rizal *et al.*, 2012). This shift could be used to trace the source of sediments that are deposited in study area.

There are two sediments sources for the site location: Asia mainland and Indonesia Maritime Continent. One of major river that flows into Andaman Sea is Irawaddy River. This river carries weathering product of rocks from Myanmar and adjacent area. The majority of Irawaddy River occurs during summer to late autumn and reaches its peak on October or two months after maximum rainfall within the Irawaddy Waterhed (Rashid *et al.*, 2007). Contrastingly, the northern part of Sumatera and Malayan Peninsula experience two maximum precipitation annually that occur on October – November and March – May (Aldrian dan Susanto, 2003). The resulted runoff allow transportation of sediments from Sumatera and Indonesian Seas.

METHODS

This study used sediment core BS-36 that was acquired by gravity corer during BENTHIC cruise 2014 on board RV Geomarin III. The 370 cm core is located off the northeast coast of Sumatra in Mergui Basin in the southeast edge of Andaman Sea (6 55,85' Sand 96 7,48' E) at 1147.1 m water depth.

Detrital, biogenic and authigenic contents in marine sediments would affect physical and chemical characteristics, such as grain size and sediment composition. Investigation of sediment composition

might involve the most simple observation using binocular microscope to highly sophisticated elemental measurement using various type of mass spectrometer. Most of the analyses either low expense but time consuming or expensive and time consuming and involved sample destruction. Core scanning using multi-sensor core logger (MSCL) is an option that offer fast, non-destructive and high resolution measurement of sediment properties including colour, magnetic susceptibility and elemental content. Core scanning result can be used to understand climate fluctuation such as presented by Permanawati *et al.* (2016) from Kangean Water and Hendrizan *et al.* (2016) from Sulawesi Sea.

This study employed core description and observation, core scanning by multi-sensor core logger (MSCL-S) Geotek and measurement of carbonate content. Core description and observation as well as core scanning were conducted at Core Repository of the Marine Geological Institute of Indonesia in Cirebon, and carbonate measurement was carried out at *First Institute of Oceanography* (FIO) in Qingdao by Vario EL III Elementar. Before measurement, samples are oven dried at 60 C for 2 hours and then ground in an agate mortar to homogenize the samples. Core scanning was performed on a split core with 1 cm resolution for magnetic susceptibility, color spectrophotometer dan X-ray fluorescence (XRF).

Magnetic susceptibility is the response of magnetic mineral to external magnetic field (Skrede, 2012) and its value would be determined by magnetic

mineral content (Nielsen and Rasmussen, 2002). Magnetic susceptibility has been applied in paleoceanography and paleoclimate studies to correlate sedimentary sequence, determine sediment condition (missing or disturb layer), and reconstruct past climate and oceanography conditions (Verosub and Roberts, 1995; Hounslow and Maher, 1999 in Larrasoana *et al.*, 2008). Magnetic susceptibility measurement is conducted by point sensor Bartington MS2E.

Colour spectrophotometry is a sensor within MSCL-S system that quantify the color of visible light spectrum. The measurements are reported as light and dark, red and green and yellow and blue that compose CIE L* a* b* classification (Fairchild, 2005). Sediment color reflects its composition and it has been employed to estimate sediment and mineralogy composition (Balsam and Damuth, 2000). An example of the application of sediment color in estimating elemental composition is the ratio of 700/400 that reflects Fe content (Wei *et al.*, 2014). This study used Konica-Minolta CM2600d colour spectrophotometer.

X-ray fluorescence (XRF) spectrometry is non-destructive method to measure elemental content of sediments. The data could be used to understand paleoenvironmental changes in Japan Sea (Yao *et al.*, 2012), identify past climate in Africa (Itambi *et al.*, 2009) and changes in marine productivity in Chile (Rebolledo *et al.*, 2008). The XRF spectrometer employed in this study is XRF Olympus Delta X. Data analysis involves calculating correlation coefficient, and principle component analysis (PCA) to determine the main factors affecting the sediments. Correlation coefficient and PCA were calculated by PAST (Hammer *et al.*, 2001).

RESULTS

Lithology

Core BS-36 is composed mostly of clay and silt with a layer of foraminiferal sand near the bottom. The color shows lightening upward trend while 700/400 ratio shows rapid increase at 270 cm. L* values fluctuates around 35 from 370-270 cm before increase abruptly to reach 41 and fluctuates around 38 to the top. The ratio of 700/400 spectrum shows increase from 1.4 to 2.1 from 370-50 cm before it drops abruptly to 1.7 and then increase upward to 2.1 to the upper part. Overall, based on lithology, L* and 700/400 ratio, core BS-36 can be divided into five units. Detailed description of each unit from bottom to top is as follows (Figure 3):

- Unit V

Unit V is characterized by gray (5Y 3/1) foraminifera-bearing clay and L* value show

similar pattern to 700/400 ratio. The values of L* fluctuate between 30.4 and 35, while the range of 700/400 values is 1.3 – 1.6. This unit composes the lower part of core BS-36 and found between 351 - 371 cm.

- Unit IV

Unit IV is formed by gray (5Y4/3) sand that contains abundant foraminifera with L* values follow 700/400 ratio. L* values fluctuate between 32.7 and 38.1, while the range of 700/400 values is 1.5 – 1.8. Unit IV is found between 332 and 350 cm.

- Unit III

Unit III is characterized by gray (5Y3/1 and 5Y4/3) clay that consists of foraminifera and exhibits inverse relationship between L* and 700/400 ratio. The range of L* values is 32.5 - 42.7, while 700/400 values fluctuate between 1.5 and 1.9. Unit III can be divided into 2 sub-units, sub-unit A that comprises of clay with high L* value and low 700/400 ratio and sub-unit B that shows opposing characteristics to sub-unit A. This unit is found between 86 and 325 cm.

- Unit II

Unit II is found between 51 and 85 cm and it composed of gray (5Y 3/1) clay comprises foraminifera and pteropods. L* values show linear relationship with 700/400 ratio with L* values range between 35.7 and 40.6 while 700/400 values fluctuate between 1.6 and 2.0.

- Unit I

Unit I form the top 50 cm of core BS-36 and it is dominated by silt. This unit has inverse relationship between L* and 700/400 ratio, with L* values range between 34.3 and 42.4 while 700/400 values range between 1.7 and 2.2. Core observation reveals color fluctuation between 5Y 4/3 and 5Y 3/2 that supports variation of measured L* values.

XRF Analysis and Carbonate Measurement

The result of XRF scanning is reported in parts per million or ppm. To avoid matrix effects, elemental content is presented as natural logarithmic (ln) ratio of said element to a major element following Weltje and Tjallingii (2008). Two ratios that have been used in understanding depositional environment are ln (Ti/Ca) and ln (Mn/Cl). The ln (Ti/Ca) was used by Fraser *et al.* (2014) as an indicator of precipitation, while ln (Mn/Cl) was interpreted as related to paleoredox condition by Yao *et al.* (2012).

To understand the relationship between elements, carbonate, and color, we calculate their correlation

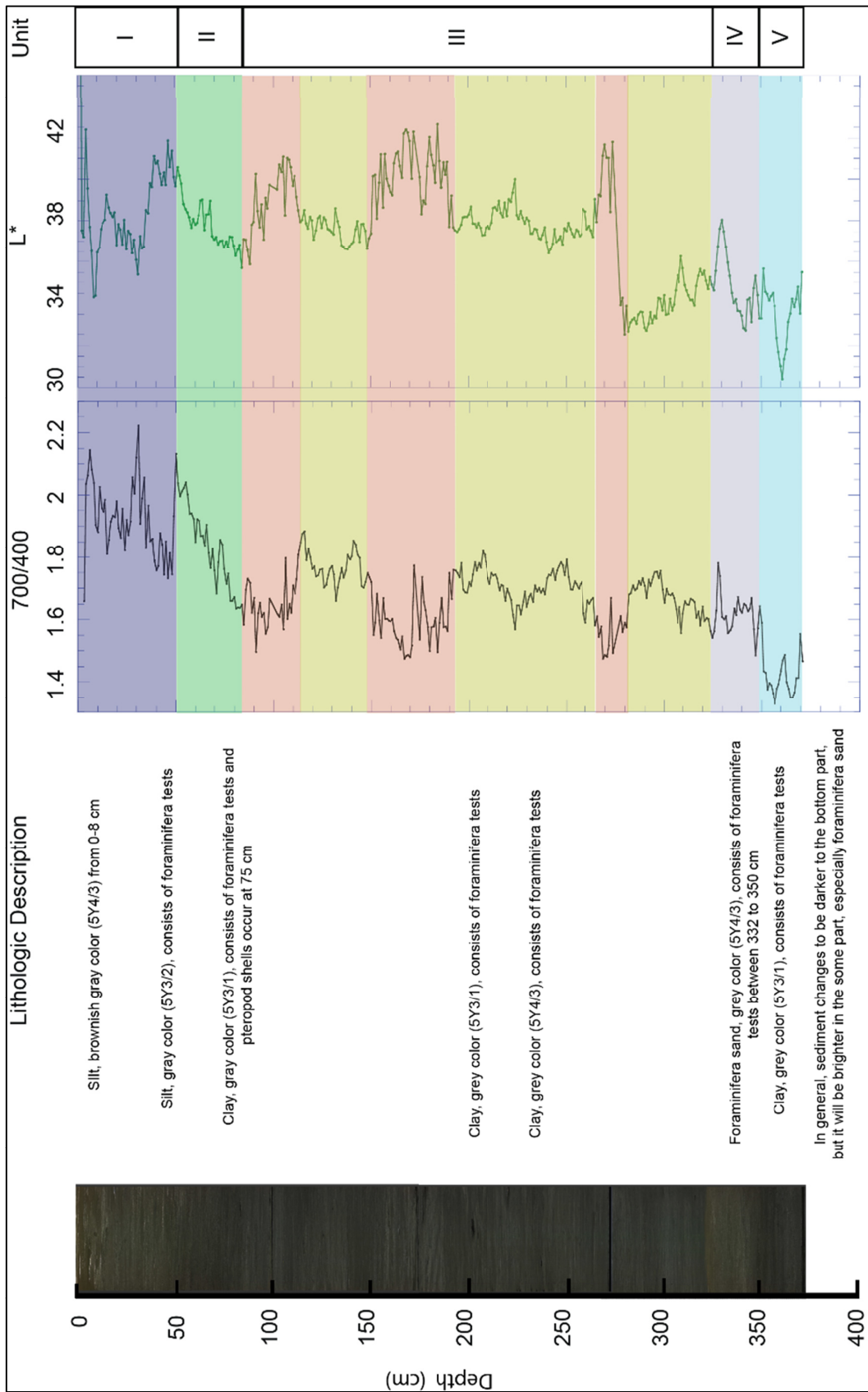


Figure 3. Lithologic unit of Core BS-36 and its physical characteristics represented by 700/400 ratio and lightness (L*).

coefficient (Table 1). Chlor shows relatively high correlation with L^* and b^* (>0.6) that suggest the effect of pore water content, indicated by Cl, to sediment color (Yao *et al.*, 2012). A strong correlation is shown by Ti and Mn (0.8) that indicates possible terrigenous source of Mn, even though Mn precipitation in most seafloor is influenced by oxygen content (Yao *et al.*, 2012). This interpretation is supported by negative correlation between Ti and Mn to carbonate content (Table 1). A relatively strong negative correlation is exhibited by $\ln(Mn/Cl)$ and carbonates that might be related to the effect of redox condition to carbonate shell preservation (Cranston and Buckley, 1990).

Combination of $\ln(Ti/Ca)$ and $\ln(Mn/Cl)$ to carbonate content and b^* value to lithology unit reveals that each lithology unit of core BS-36 has distinct characteristic (Figure 4). In general, $\ln(Ti/Ca)$ shows decreasing upward trend with three maxima at 325-310, 160-150 cm and 60-40 cm, while b^* exhibit increasing upward trend. An inverse pattern is shown by $\ln(Mn/Cl)$ and carbonate content.

Unit V is signified by decreasing upward $\ln(Ti/Ca)$ and b^* , while $\ln(Mn/Cl)$ relatively stable and carbonate content slightly increase. The range of values for $\ln(Ti/Ca)$, b^* , $\ln(Mn/Cl)$ and carbonate are: -4.5 to -3.7; 4.2 to 5.9; -7.5 to -6.9; and 19.7 to 32.9.

Table 1. Correlation coefficient between physical and chemical properties of marine sediments from Andaman Sea.

	Cl (ppm)	Ca (ppm)	Ti (ppm)	Mn (ppm)	$\ln(Ti/Ca)$	$\ln(Mn/Cl)$	L^*	b^*	Carbonate (%)
Cl (ppm)									
Ca (ppm)	0.34603								
Ti (ppm)	-0.16545	0.55143							
Mn (ppm)	0.059856	0.58491	0.82583						
$\ln(Ti/Ca)$	-0.51299	-0.70245	0.17916	0.019671					
$\ln(Mn/Cl)$	-0.38428	0.40226	0.82481	0.88454	0.2164				
L^*	0.68646	0.22089	-0.12744	0.022625	-0.30398	-0.23998			
b^*	0.67608	0.12142	-0.275	-0.18717	-0.32433	-0.45389	0.6938		
Carbonate (%)	0.18517	-0.12717	-0.57784	-0.63394	-0.29586	-0.66913	0.057084	0.30144	

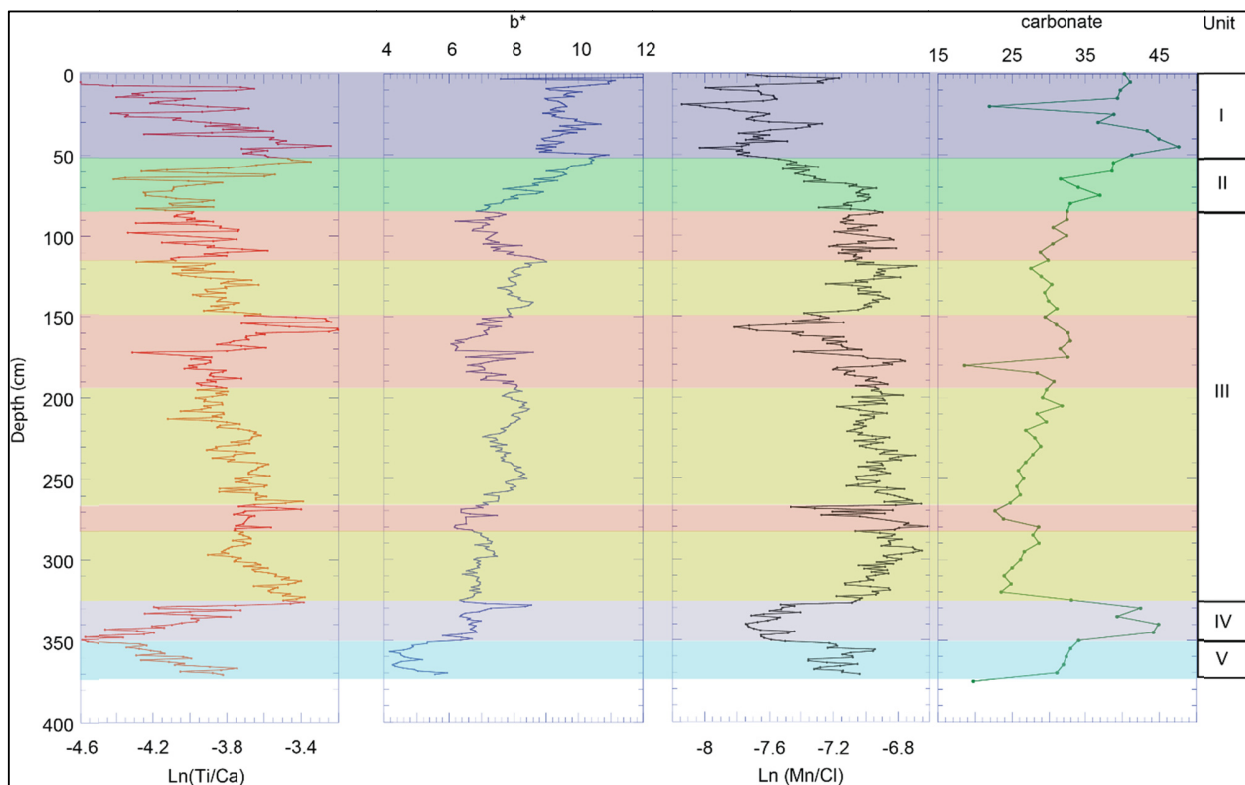


Figure 4. Correlation between lithology and physical properties measured by MSCL and carbonate content.

Unit IV is characterised by sharp increase of $\ln(\text{Ti}/\text{Ca})$, b^* , $\ln(\text{Mn}/\text{Cl})$ and carbonate content. The range of values for $\ln(\text{Ti}/\text{Ca})$, b^* , $\ln(\text{Mn}/\text{Cl})$ and carbonate are: -4.6 to -3.4; 5.8 to 8.6; -7.7 to -7.1; and 34 to 44.9. Carbonate content in Unit IV reaches its first peak that is only slightly lower than the second peak that is observed in the upper part (Unit I).

Unit III demonstrate fluctuations of $\ln(\text{Ti}/\text{Ca})$, b^* , $\ln(\text{Mn}/\text{Cl})$, and carbonate content with an overall trend of decreasing upward. The values of $\ln(\text{Ti}/\text{Ca})$ range between -4.3 and -3.2, b^* range between 6.1 and 9, $\ln(\text{Mn}/\text{Cl})$ range between -7 and -6.6, and carbonate content range between 18.6 and 33. The maximum value of $\ln(\text{Ti}/\text{Ca})$ occurs at 160-150 cm concurrent with minimum value of $\ln(\text{Mn}/\text{Cl})$. An interesting feature of this unit is the similarities of b^* fluctuation to 700/400 (Figure 3) that indicate the importance of redox condition to Fe content.

Unit II is indicated by increasing $\ln(\text{Ti}/\text{Ca})$, b^* and carbonate content, with values range between -4.4 and -3.3, 6.8 and 10.5, 31.5 and 41.2, respectively. Contrasting trend is shown by $\ln(\text{Mn}/\text{Cl})$ that is decreasing upward with values range between -7.7 and -6.9.

Unit I is characterised by decreasing values of $\ln(\text{Ti}/\text{Ca})$ and increasing values of $\ln(\text{Mn}/\text{Cl})$, 04.7 to -3.2 and -8.1 to -7.2 respectively. The values of b^* range between 7.6 and 11.1, while carbonate content range between 21.9 and 47.6.

DISCUSSION

L^* value has been applied as indicator of carbonate content in the Gulf of Cadiz sediment by Rogerson *et al.* (2006). However, carbonate content of BS-36 show similar trend to b^* instead of L^* (Figures 3 and 4) with higher correlation coefficient to b^* than to L^* (Table 1). This discrepancy points to the effect of redox condition to shell preservation in marine sediment as was considered in previous section.

Beside carbonate content, light colored sediments might reflect high content of Si, Sr and Zr as was observed by Sprenk *et al.* (2014) in Weddell Sea. The source of silica in Andaman Sea sediments are considered to be the granite belt of Malaya Peninsula and volcanic rocks of northern Sumatra (Crow and Barber, 2005) or Andaman islands (Awasthi, 2012 and Awasthi *et al.*, 2010). Surface circulation pattern in the study area shows north- and northeastward flows from the south to core location (Rizal *et al.*, 2012) that made transport of silica from Malay Peninsula or Andaman islands to core BS-36 location negligible.

Better correlation of carbonate content to b^* than L^* in core BS-36 along with possible negligible silica input suggests that redox plays an important role in determining carbonate content in this location. Further

study on foraminiferal assemblage should take this condition into account.

Another factor that influence carbonate content is productivity that is affected by terrigenous input. Sediment transport from the land to the sea in this region is mostly dominated by runoff, particularly river runoff that is influenced by precipitation on land. Carbonate content of core BS-36 shows inverse trend to $\ln(\text{Ti}/\text{Ca})$, an indicator of precipitation, from Unit V to Unit II but similar trend in Unit I. Contrastingly, carbonate content of Unit V and I shows similar trend to $\ln(\text{Mn}/\text{Cl})$ but reverse trend for Units II to IV. This condition suggests change in predominant factor that influences carbonate content.

Fluctuations of Environmental Condition during Deposition

Multi-proxy analyses on Core BS-36 reveal five distinct environmental conditions. Changes in depositional environments in study area consist of variation of bottom oxygenation (anoxic – oxic), precipitation and productivity rate. The discussion of these changes are described from bottom (Unit V) to top (Unit I) of the core to reflect sedimentary sequences.

Units V and IV show darker sediment color, low $\ln(\text{Ti}/\text{Ca})$ and high carbonate content (Figs. 3 and 4). This characteristics might be related to low precipitation with high productivity that resulted in high carbonate producing organisms. The darker sediment color is inferred to reflect higher Fe content following Guimaraes *et al.* (2013) that might be deposited in suboxic to anoxic condition signified by low $\ln(\text{Mn}/\text{Cl})$ value that according to Yao *et al.* (2012) indicates paleoredox condition.

Unit III is interpreted to be deposited during relatively high precipitation ($\ln \text{Ti}/\text{Ca}$) that provided adequate runoff to carry Si-rich terrigenous material from Malay Peninsula to core location. The transport of Si-rich terrigenous material from Malay Peninsula into core location might happen during NE Monsoon when watermass from Malacca Strait pushes the Indian Ocean water into the northern border of the Andaman Sea as presented by Rizal *et al.* (2012). The presence of Si-rich sediments in core BS-36 implies weakening of Indian Monsoon during the sedimentation of unit III. The weakening of Indian Monsoon reaches its minima in the end of unit III deposition. This unit is interpreted as deposited in oxic condition that might be the result of better ocean ventilation producing bottom oxygenation.

Rapid increase of precipitation might occur during the deposition of the lower part of Unit II and reached its peak early on Unit I deposition before slowly decreased. Increased of precipitation occurred simultaneously with increased carbonate production, slow-down of ocean circulation that resulted in suboxic

to anoxic condition of core BS-36 location that yielded Fe-rich sediments of Units I and II.

CONCLUSION

Physical and chemical properties along with carbonate content has been analysed from core BS-36 from Andaman Sea. The results show that the sediments can be classified into 5 lithologic units based on lithology, color and elemental contents. The characteristics of each unit reveal changes in depositional environment condition. The bottom part of the core was deposited during suboxic to anoxic bottom condition combined with high productivity and low precipitation, going upward the depositional condition changed into a high precipitation and oxic condition due to ocean ventilation, then the condition changed into higher precipitation, higher carbonate production and suboxic to anoxic condition.

ACKNOWLEDGEMENT

This study is funded by the Analysis of the Characteristic of Deep Water Resources Research Project of the Marine Research Center (MRC), ARHRMF, Ministry of Marine Affairs and Fisheries (MMAF), 2015. This project involved scientists from MRC, Marine Geological Institute of Indonesia (MGI), ARDEMR, MEMR, and Research Center for Geotechnology (RCG) LIPI. The authors are grateful to all BENTHIC cruise participants who worked hard on acquiring the sediment core that is presented in this paper. We appreciate the Captain and crew of Geomarin III that carried out the BENTHIC cruise, a collaboration between the Marine Geology Division of the First Institute of Oceanography (FIO), SOA, China and MMAF. The authors would like to thank the Director of P3SDLP who supported to this research. We would also like to thank the Directors of MGI, RCG-LIPI, and Prof. Xuefa Shi and Dr. Shengfa Liu who supported this study.

REFERENCES

- Aldrian, E., and Susanto, R.D. 2003. Identification of three dominant rainfall regions within Indonesia and their relationship to sea surface temperature, *International Journal of Climatology* 23, 1435–1452.
- Anderson, O.R. 1983. *Radiolaria*. Springer-Verlag, New York, 355 p.
- Awasthi, N. 2012. *Geochemical and Isotopic studies of sediments from the Andaman Islands and the Andaman Sea*. PhD thesis, M.S. Univ. of Baroda, Vadodara, India.
- Awasthi, N., Ray, J.S., Laskar, A.H., Kumar, A., Sudhakar, M., Bhutani, R., Sheth, H.C., and Yadava, M.G. 2010. Major ash eruptions of Barren Island volcano (Andaman Sea) during the past 72 kyr: Clues from a sediment core record. *Bulletin of Volcanology*, 72:1131–1136.
- Awasthi, N., Ray, J.S., Singh, A.K., Band, S.T., and Rai, V.K. 2014. Provenance of the Late Quaternary sediments in the Andaman Sea: Implications for monsoon variability and ocean circulation. *Geochemistry, Geophysics, Geosystem*, 15:3890–3906, doi: 10.1002/2014GC005462.
- Balsam, W.L., and Damuth, J.E. 2000. Further Investigations of Shipboard vs Shore-Based Spectral Data: Implications for Interpreting Leg 164 Sediment Composition, in Paull, C.K., Matsumoto, R., Wallace, P.J., and Dillon, W.P. (Eds.): *Proceeding ODP, Scientific Results, 164*. College Station, TX (Ocean Drilling Program).
- Boles, J.R. 2014. *Authigenic minerals* in Access Science. McGraw-Hill Education. <http://dx.doi.org/10.1036/1097-8542.062800>.
- Cranston, R.E., and Buckley, D.E. 1990. Redox reactions and carbonate preservation in deep-sea sediments. *Marine Geology*, 94:1-8.
- Crow, M.J. and Barber, A.J. 2005. Simplified geological map of Sumatra. In: Barber, A.J., Crow, M.J., dan Milsom, J.S. (eds.) *Sumatra Geology, Resources and Tectonic Evolution. Geological Society Memoir*, 31. doi:10.1144/GSL.MEM.2005.031.01.17.
- Fairchild, M.D. 2005. *Color and Image Appearance Models. Color Appearance Models*. John Wiley and Sons. 340 p.
- Fraser, N., Kuhnt, W., Holbourn, A., Bolliet, T., Andersen, N., Blanz, T., and Beaufort, L. 2014. Precipitation variability within the West Pacific WarmPool over the past 120 ka: Evidence from the Davao Gulf, southern Philippines. *Paleoceanography*, 29:1094–1110, doi: 10.1002/2013PA002599.
- Guimaraes, J.T.F, Cohen, M.C.L., Franca, M.C., da Silva, A.K.T., and Rodrigues, S.F.S. 2013. Mineralogical and geochemical influences on sediment color of Amazon wetlands analyzed by visible spectrophotometry. *Acta Amazonica*, 43:331 – 342.
- Gupta, K.S. 1999. *Modern Foraminifera*. Springer, Dordrecht, 279p.
- Gustiantini, L., Maryunani, K.A., Zuraida, R., Kissel, C., Bassinot, F., and Zaim, Y. 2015. Distribusi

- foraminifera di Laut Halmahera dari glasial akhir sampai resen (foraminiferal distribution since the last glacial until recent in Halmahera Sea), *Jurnal Geologi Kelautan*, 13(1): 25-36.
- Hall., R. and Morley, C. 2004. Sundaland Basin, in Clift, P. D., Wang, P., Kuhnt, W., and Hayes, D. (Eds.), *Continent-Ocean Interactions within the East Asian Marginal Seas: Geophysical Monograph 149*. Washington, D.C.: American Geophysical Union, 55-85.
- Hammer, O., Harper, D.A.T., and Ryan, P.D. 2001. PAST: Paleontological Statistics Software Package for Education and Data Analysis. *Palaeontologia Electronica*, 4:9. (<http://folk.uio.no/hammer/past>).
- Hemming, S. R., van de Flierdt, T., Goldstein, S.L., Franzese, A.M., Roy, M., Gastineau, G., and Landrot, G. 2007. Strontium isotope tracing of terrigenous sediment dispersal in the Antarctic Circumpolar Current: Implications for constraining frontal positions. *Geochemistry, Geophysics, Geosystem*, 8:Q06N13, doi:10.1029/2006GC001441.
- Hendrizan, M., Zuraida, R., and Cahyarini, S.Y. 2016. Karakteristik Sedimen Palung Laut Sulawesi (Sumur St12) berdasarkan Hasil Pengamatan Megaskopis dan Sifat Fisika dari Pengukuran Multi-Sensor Core Logger (MSCL). *Riset Geologi dan Pertambangan*, 26: 69-80. doi: 10.14203/risetgeotam2016.v26.273.
- Itambi, A.C., von Dobeneck, T., Mulitza, S., Bickert, T., and Heslop, D. 2009. Millennial-scale northwest African droughts related to Heinrich events and Dansgaard-Oeschger cycles: Evidence in marine sediments from offshore Senegal. *Paleoceanography*, 24: PA1205, doi: 10.1029/2007PA001570.
- Kraal, P., Slomp, C. P., Reed, D.C., Reichert, G.-J., and Poulton, S. . 2012. Sedimentary phosphorus and iron cycling in and below the oxygen minimum zone of the northern Arabian Sea. *Biogeoscience*, 9:2603–2624, doi:10.5194/bg-9-2603-2012.
- Larrasoana, J.C., Roberts, A.P., and Rohling, E.J. 2008. Magnetic susceptibility of eastern Mediterranean marine sediments as a proxy for Saharan dust supply? *Marine Geology*, 254:224–229.
- Lin, Y. N., Sieh, K., and Stock, J. 2010. Submarine landslides along the Malacca Strait? Mergui Basin shelf margin: Insights from sequence?stratigraphic analysis. *Journal of Geophysical Research*, 115:B12102, doi:10.1029/2009JB007050.
- Millot, G., 1970. *Geology of Clays: Weathering, Sedimentology, Geochemistry*. Springer-Verlag Paris, 427 p.
- Nielsen, B.M., and Rasmussen, T.M. 2002. Geological correlation of magnetic susceptibility and profiles from Nordre Strømfjord, southern West Greenland. *Geology of Greenland Survey Bulletin*, 191:48–56.
- Permanawati, Y., Prartono, T., Atmadipoera, A.S., Zuraida, R., and Chang, Y. 2016. Rekam sedimen inti untuk memperkirakan perubahan lingkungan di perairan lereng Kangean (core sediment records to predict environmental changes in Kangean slope Waters). *Jurnal Geologi Kelautan*, 14(2): 65-77.
- Rahman, M.A. and Oomori, T. 2008. Structure, crystallization and mineral composition of sclerites in the alcyonarian coral. *Journal of Crystal Growth*, 310(15): 3528-3534.
- Rashid, H., Flower, B.P., Poore, R.Z., and Quinn, T.M. 2007. A ~ 25 ka Indian Ocean monsoon variability record from the Andaman Sea. *Quaternary Science Review*, 26:2586–2597.
- Razali, M. 2011. Play type in the cross border North Sumatra – Mergui Basin. *North Sumatra – Mergui Basin Cross Border Case Study EPPM-CCOP*, 1-44.
- Rebolledo, L., Sepulveda, J., Lange, C.B., Pantoja, S., Bertrand, S., Hughen, K., and Figueroa, D. 2008. Late Holocene marine productivity changes in Northern Patagonia-Chile inferred from a multi-proxy analysis of Jacaf channel sediments. *Estuarine, Coastal and Shelf Science*, 80:314–322.
- Rizal, S., Damm, P., Wahid, M.A., Sundermann, J., Ilhamy, Y., Iskandar, T., and Muhammad. 2012. General Circulation in the Malacca Strait and Andaman Sea: a Numerical Model Study. *American Journal of Environmental Science*, 8:479-488.
- Rogerson, M., Weaver, P.E., Rohling, E.J., Lourens, L.J., Murray, J.W., and Hayes, A. 2006. Colour logging as a tool in high-resolution palaeoceanography, in: Rothwell R.G. (ed.) *New Techniques in Sediment Core Analysis*. Geological Society. London: Special Publications, 267:99-112.
- Skrede, K. 2012. *Magnetic susceptibility of sedimentary rocks from Bjørnøya*. Thesis.

Norwegian University of Science and Technology. Unpub.

- Spooner, M. I., Barrows, T. T., De Deckker, P., and Paterne, M. 2005. Palaeoceanography of the Banda Sea, and Late Pleistocene initiation of the Northwest Monsoon. *Global Planetary Change*, 49:28-46, doi:10.1016/j.gloplacha.2005.05.002.
- Sprenk, D., Weber, M.E., Kuhn, G., Wennrich, V., Hartmann, T., and Seelos, K. 2014. Seasonal changes in glacial polynya activity inferred from Weddell Sea varves. *Climate of the Past*, 10:1239–1251. doi:10.5194/cp-10-1239-2014.
- Troa, R.A., Liu, S., Zuraida, R., Triarso, E., Gustiantini, L., and Hendrizan, M. 2014. *Cruise Report of BENTHIC Cruis Phase I*. Research and Development Center for Marine and Coastal Resources – Ministry of Marine Affairs and Fisheries. 40 p. Unpublished report.
- Tripathi, S.K. 2014. Biogenic sediment distribution around south of Central Andaman Trough, Andaman Sea: signatures from micropaleontological studies. *Indian Journal of Geoscience*, 68:337-346.
- Wei, J.H., Finkelstein, D.B., Brigham-Grette, J., Castaneda, I.S., and Nowaczyk, N. 2014. Sediment colour reflectance spectroscopy as a proxy for wet/dry cycles at Lake El'gygytyn. Far East Russia, during Marine Isotope Stages 8 to 12. *Sedimentology*, 61:1793-1811.
- Weltje, G.J. and Tjallingii, R. 2008. Calibration Of XRF Core Scanners For Quantitative Geochemical Logging Of Sediment Cores: Theory And Application. *Earth and Planetary Science Letter*, 274:423–438.
- Yao, Z., Liu, Y., Shi, X., and Suk, B.-C. 2012. Paleoenvironmental changes in the East/Japan Sea during the last 48 ka: indications from high-resolution X-ray fluorescence core scanning. *Journal of Quaternary Science*, 27:932-940.